

Robust Identity Perceptual Watermark Against Deepfake Face Swapping

Tianyi Wang¹ Mengxiao Huang^{2,3} Harry Cheng⁴ Bin Ma^{2,3,*} Yinglong Wang^{2,3,*}

¹Nanyang Technological University, Singapore ²Qilu University of Technology, China

³Shandong Academy of Sciences, China ⁴Shandong University, China

Abstract

Notwithstanding offering convenience and entertainment to society, Deepfake face swapping has caused critical privacy issues with the rapid development of deep generative models. Due to imperceptible artifacts in high-quality synthetic images, passive detection models against face swapping in recent years usually suffer performance damping regarding the generalizability issue. Therefore, several studies have been attempted to proactively protect the original images against malicious manipulations by inserting invisible signals in advance. However, the existing proactive defense approaches demonstrate unsatisfactory results with respect to visual quality, detection accuracy, and source tracing ability. In this study, to fulfill the research gap, we propose the first robust identity perceptual watermarking framework that concurrently performs detection and source tracing against Deepfake face swapping proactively. We assign identity semantics regarding the image contents to the watermarks and devise an unpredictable and nonreversible chaotic encryption system to ensure watermark confidentiality. The watermarks are encoded and recovered by jointly training an encoder-decoder framework along with adversarial image manipulations. Falsification and source tracing are accomplished by justifying the consistency between the content-matched identity perceptual watermark and the recovered robust watermark from the image. Extensive experiments demonstrate state-of-the-art detection performance on Deepfake face swapping under both cross-dataset and cross-manipulation settings.

1. Introduction

The prevalent Deepfake face swapping technique has received widespread attention with the development of deep generative models. By swapping the facial identity from the source image onto the target one, Deepfake face swapping can bring convenience to people’s lives and benefit society from the perspective of human entertainment such

as film-making. Nevertheless, misusing the technique has brought privacy issues to various groups of victims including celebrities, politicians, and even every human being [47]. Therefore, it is necessary to prevent malicious attacks while maintaining positive usages of Deepfake face swapping.

Most existing countermeasures [13, 22, 33, 35, 38, 46, 50, 60] regarding Deepfake face swapping follow the pipeline of devising a deep detection model that passively investigates and analyzes the underlying synthetic artifacts to distinguish the fake images. While accomplishing progresses in the early stages, passive detection suffers the generalization challenge such that obvious performance damping occurs when attempting to detect fake materials produced by unknown synthetic algorithms [45]. Moreover, following rapid improvements in deep generative algorithms, it has become burdensome to locate perceivable manipulation traces within high-quality synthetic images. To overcome this issue, several recent studies consider executing proactive defense against synthetic manipulations. In other words, the goal is to protect the original images by inserting imperceptible signals in advance of posting in public and being manipulated by Deepfake unexpectedly.

The proactive approaches can be categorized into two main strategies, namely, distorting [15, 44, 48] and watermarking [3, 25, 30, 31, 55]. The former learns a distortion that nullifies potential synthetic manipulations by inserting it into the original images, and the latter encodes semi-fragile watermarks into original images and determines the authenticity based on the existence of watermarks afterward. Both ways aim to proactively protect the original images without affecting the visual qualities. While demonstrating preliminary initiations, the existing approaches suffer several flaws. Firstly, in the current research stage, both the distorting and watermarking approaches lack generalization ability on unseen datasets when facing unknown synthetic manipulations. Secondly, although the semi-fragile watermarks can help determine real and fake based on their existence, they are prone to be unstable when facing unavoidable common image processing operations. Moreover, watermarks that are fragile to malicious synthetic ma-

*Corresponding authors: Yinglong Wang and Bin Ma.

nipulations cannot help conduct source tracing on the victim target images simultaneously. In particular, in an integral chain of evidence for the forensic investigation in the cybercrime cases related to Deepfake face swapping, besides correctly addressing the falsification, it is crucial to retrieve intelligence information of the source materials [1, 20, 51]. In other words, tracing the original target images along with the detection task can help fulfill the evidence integrality. Lastly, while preventing privacy issues, directly adding distortions not only unavoidably degrades the visual qualities of the images [11], but also unfavorably disables benign adoptions of Deepfake face swapping.

To address the aforementioned issues, in this study, we propose a novel robust identity perceptual watermarking framework that promotes proactive defense against Deepfake face swapping. In general, we establish semantically meaningful identity perceptual watermarks that are robust and invisible based on image contents and embed them into original images for detection and source tracing purposes simultaneously, while allowing benign usages of face swapping algorithms. First, based on the identities of facial images, we construct securely protected identity perceptual watermarks by introducing a chaotic encryption system. Then, we devise an end-to-end robust watermarking framework that consists of an encoder-decoder architecture to be trained with common and face swapping manipulation pools. Relying on the promising watermark recovery performance, the authenticity of a candidate image is determined by the consistency between the content-matched identity perceptual watermark and the robustly recovered watermark from the image. The source tracing is simultaneously achieved with respect to the identity semantics carried by the recovered watermark. Extensive experiments prove the generalization ability of our proposed approach under cross-dataset and cross-manipulation settings with average watermark recovery accuracies all above 96%, strongly outperforming the contrastive methods. The outstanding detection performance against Deepfake face swapping with AUC scores all above 97% also consistently outperforms the state-of-the-art passive Deepfake detectors.

Our contributions can be summarized as follows:

- We propose a novel idea of identity perceptual watermarks based on image contents to proactively defend against Deepfake face swapping regarding content-watermark consistencies. A chaotic encryption system is collaboratively devised to ensure watermark confidentiality.
- We present an encoder-decoder framework to robustly and invisibly embed the watermarks into facial images. To the best of our knowledge, we are the first to concurrently achieve detection and source tracing for Deepfake face swapping by embedding a single watermark.
- Experiments qualitatively and quantitatively demonstrate

the promising watermark recovery accuracy and Deepfake face swapping detection performance of our method along with outstanding generalization ability, outperforming the related state-of-the-art algorithms.

2. Related Work

Existing forensic investigations on Deepfake face swapping mostly rely on devising passive detectors [13, 22, 32, 33, 38, 50, 60] that analyze traces of suspected images in various feature domains. In view of the rising challenge prompted by the improving synthetic quality, instead of searching for synthetic artifacts, proactive defense aims to protect original images by inserting imperceptible signals before potential manipulations. In other words, while malicious face swapping happens after the target image is publicly posted (e.g., on Twitter or Instagram), proactive actions are performed in advance in two ways: *distortions* and *watermarks*.

2.1. Proactive Distortions

Proactive distortions [2, 17, 37, 56, 57] are usually inserted into pristine images to nullify the synthetic models following $\tilde{x} = x + \eta$, where x and \tilde{x} are the pristine images before and after the learned invisible distortion η is added, respectively. In particular, recently, Anti-Forgery [44] exploits the vulnerability of GAN-based models and supervises learns a particular distortion in the lab color space for a specific pristine image regarding each synthetic algorithm. CMUA [15] presents a two-level perturbation fusion strategy and heuristically learns a universal distortion that can disrupt multiple synthetic algorithms. TAFIM [2] introduces image-specific perturbations with better robustness via attention-based fusion and refinement. Besides adding invisible perturbations that could heavily distort the synthetic results, Wang *et al.* [48] further promoted a detector that distinguishes the distorted images with high accuracy since machines do not share similar perspectives as human eyes.

2.2. Proactive Watermarks

Digital watermarks [41] are originally used for copyright protection and authentication [9, 23, 54], and they are thus designed to have promising robustness. Ever since the occurrence of the first deep neural network (DNN) based end-to-end trainable watermarking framework, HiDDeN [61], various follow-up algorithms [8, 16, 18, 28, 40] emerge based on the encoder-decoder architecture for robust watermarking. The encoder reconstructs a visually identical image by inserting a secret message into the original one, and the decoder takes charge of recovering the encoded message from the watermarked image. Particularly, MBRS [18] proposes a novel training strategy within mini-batches to enhance the JPEG robustness of watermark embedding. To

simultaneously improve watermark imperceptibility and robustness against unknown image noises, CIN [28] combines the invertible and non-invertible mechanisms in the watermark embedding and recovery pipelines. ARWGAN [16] enforces more abundant features from images for robust watermarking such that the image visual quality and watermark recovery accuracy can be concurrently boosted.

Regarding the relatively novel term of proactive defense, few approaches have been attempted with watermarks. Yu *et al.* [58, 59] assigned particular fingerprints to images via robust watermarking regarding generative models for the attribution purpose. Different from the robust watermarking studies, FaceGuard [55] and FaceSigns [31] propose semi-fragile watermarks such that they stay robust to benign image post-processing operations but become fragile when facing malicious face manipulations. The authors claimed to distinguish fake materials if no watermark is detected in candidate images. Recently, a separable watermarking framework, SepMark [51], is conducted with two watermark decoders, a Tracer and a Detector, where the former recovers robust watermarks for source tracing, and the latter extracts semi-fragile watermarks to determine real and fake. To the best of our knowledge, robust watermarking has been barely attempted to detect Deepfake face swapping adaptively, and performing detection and source tracing simultaneously with a single watermark remains largely unexplored in the current research domain.

3. Methodology

3.1. Overview

In this paper, we propose an identity perceptual watermarking framework to adaptively embed imperceptible robust watermarks into images and proactively achieve detection and source tracing against Deepfake face swapping by precisely recovering the encoded watermarks. The model framework is demonstrated in Fig. 1. First, we devise a watermark generator G_m to securely prepare the binary watermarks by assigning identity perceptual semantics with respect to the image contents. Then, the encoder is fed with the clean image I and the corresponding watermark m for encoding. To guarantee robustness, we apply a common manipulation pool P_{common} and a face swapping manipulation pool P_{swap} as adversaries to the watermarked image I_{rec} before recovering the watermark m_{rec} via the decoder. Meanwhile, a discriminator that distinguishes the watermarked and clean images is adopted in the training stage to enhance image visual quality. By assigning constraints as discussed in Section 3.5, the framework is trained to satisfy our objectives.

In practice, for an original image I with facial identity t , the identity perceptual watermark m is produced by G_m and embedded into I to generate the watermarked image I_{rec} via

the encoder. Upon the malicious face swapping manipulation, a synthetic facial image I_{fake} is derived by swapping identity s onto I_{rec} . By utilizing the decoder, the watermark m_{rec} which is faithfully consistent with m can be robustly recovered from I_{fake} . Since I_{fake} contains facial identity s , its corresponding watermark m_s can be generated using G_m , and demonstrating the inconsistency between m_{rec} and m_s can accomplish the detection task on Deepfake face swapping. On the other hand, as m_{rec} is robustly recovered, the trusted original image I with identity perceptual watermark m can be traced by inspecting the matchings between identities and watermarks in an officially recorded hash map.

3.2. Identity Perceptual Watermarks

Unlike early frameworks that enforce random initialization, we derive the watermark for each facial image by analyzing the identity semantics. In particular, we propose an identity perceptual watermark generator G_m that generates binary watermark m with length l based on the facial identity of image I . Inspired by hashing algorithms [24, 36], the pipeline of G_m follows two critical characteristics: *collision free* and *one-way computational*.

Collision Free. Since the goal is to detect Deepfake face swapping by addressing inconsistencies between the recovered and content-matched watermarks of candidate images, it is necessary to ensure that no two identical watermarks belong to different facial identities. Face recognition, a task to identify different facial identities by producing distinguishable embeddings, has been proved the ability on various large datasets with reliable models. In this study, impressed by the outstanding achievements, we adopt well-performed face recognition algorithms that retrieve identity embeddings in the form of high-dimensional vectors. To match up the required watermark length l , we first select a large dataset that contains sufficient unique identities and retrieve the identity embeddings E with dimension d_E accordingly. Then, we apply the principal component analysis (PCA) [34] to E and learn a transform rule ϕ that projects the identity embeddings of the images from dimension d_E down to l while optimally preserving the original correlations between facial identities with respect to the principal components. Thereafter, for the purpose of constructing binary watermarks, we conduct a unit-variance scaling on the projected embeddings E_{pca} to the range between 0 and 1 by

$$E_{\text{scale}} = \frac{E_{\text{pca}} - \min(E_{\text{pca}})}{\max(E_{\text{pca}}) - \min(E_{\text{pca}})}, \quad (1)$$

where E_{scale} denotes the scaled embeddings with respect to the standard deviation, which favorably preserves the distribution of E_{pca} . In the end, we set a cutoff value $0 \leq c \leq 1$ to round the entries of E_{scale} to binary values accordingly and obtain the identity perceptual watermarks E_{binary} . Besides,

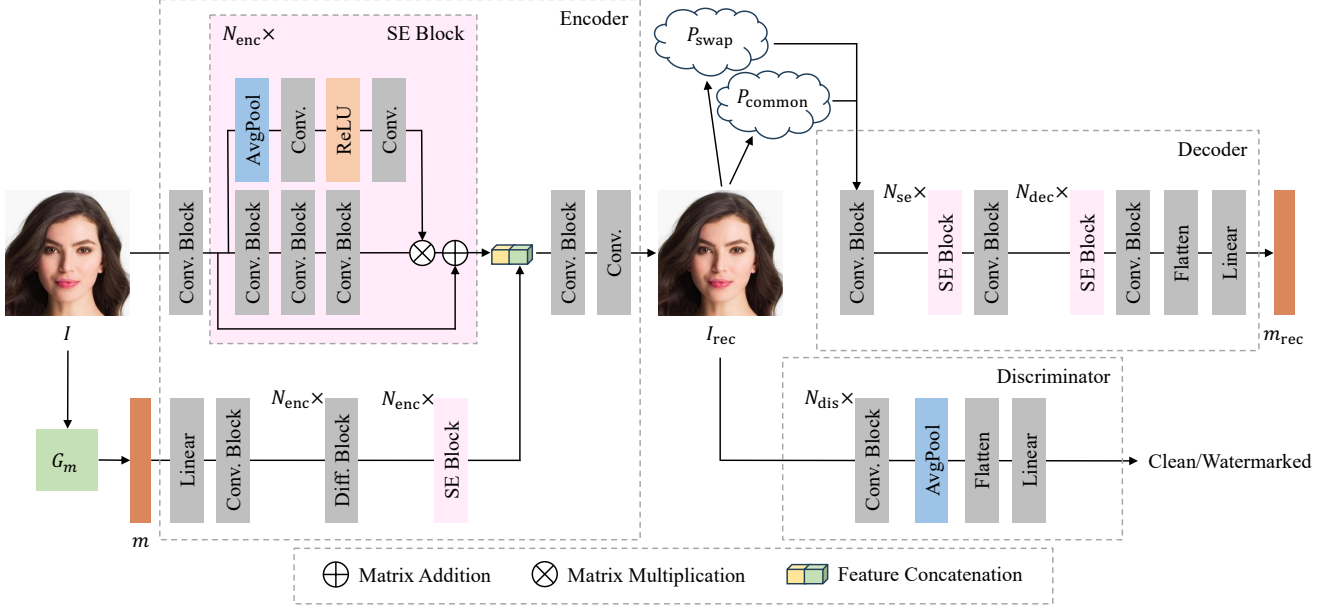


Figure 1. Framework of the proposed approach. An original clean image I is first passed to generator G_m to generate the corresponding identity perceptual watermark m . Then, I and m are fed to the encoder for watermark embedding. Manipulation pools P_{common} and P_{swap} help preserve watermark robustness during supervision. A discriminator helps maintain the visual quality. In the end, the watermark m_{rec} is recovered by passing the manipulated image to the decoder.

a watermark collision check is arranged in Section 4.4 to validate the collision-free characteristic.

One-Way Computational. Since we concurrently conduct detection and source tracing, an adversary with sufficient knowledge of our work may aim to replace the encoded watermark with a content-matched one. To prevent hostile attacks [6, 42], we enforce the watermark to be one-way computational, that is, it is insufficient to recover the watermark construction pipeline by merely acquiring the watermark from the image. Specifically, besides keeping ϕ encapsulated, we design a chaotic encryption [29] system on E_{binary} using a logistic map

$$x_{i+1} = rx_i(1 - x_i), \quad (2)$$

where constants x_0 at $i = 0$ and r are the initial condition and control parameter, respectively. x_i denotes the i -th value in the chaotic map and $0 \leq i < l$. The values in $X = \{x_1, x_2, \dots, x_l\}$ are derived accordingly, and a binary encryption key $K = \{k_1, k_2, \dots, k_l\}$ is computed via

$$k_i = \lfloor x_i p^q \bmod 2 \rfloor, \quad (3)$$

where p and q are pre-defined prime constants. Finally, the encrypted identity perceptual watermark m for image I is derived by a logical exclusive OR (XOR) operation between K and the unencrypted watermark from E_{binary} . Relying on the sensitive dependence on the initial condition and chaotic map nonlinearity characteristics, the final watermarks leveraged in the watermarking framework are unpredictable and

nonreversible unless having access to Eqn.(2) and Eqn.(3) including the critical constant coefficients. Specifically, the entry values in X vary drastically with respect to the values of x_0 and r , and the watermarks are thus securely protected. On the other hand, with authority on K , performing an extra XOR operation on m using K can easily decrypt the watermarks back to the ones in E_{scale} to trace back for the identity information.

3.3. Watermark Encoding

For an input image I , we insert the watermark m using an encoder that is mainly based on convolutional neural networks (CNN) with squeeze-and-excitation networks (SENet) [12] and diffusion blocks. Specifically, the image features and watermark features are separately analyzed and then concatenated to reconstruct the watermarked image I_{rec} .

Image Features. In this paper, we preserve the width and height of I in the propagation process to avoid information loss in image reconstruction. We first feed I to a convolutional block (denoted as Conv. Block) that contains a CNN layer, a batch normalization layer, and a ReLU activation function in a sequential order to exaggerate the number of feature channels. Squeeze-and-excitation network (SENet) [12], an on-the-shelf mechanism that improves channel interdependencies, can favorably perform feature recalibration on the input image. As depicted in Fig. 1, N_{enc} repeated SENets (denoted as SE Block) are ap-



Figure 2. Visual effects of common image manipulations on the watermarked images. The first two columns refer to the raw and watermarked images, and each of the rest rows displays the visual effects of a manipulation algorithm on the watermarked images.

plied to seek proper channels and elements within the feature map for watermark encoding without jeopardizing the visual quality.

Watermark Features. As for the binary identity perceptual watermark m of length l , we first increase the length linearly via a fully connected layer followed by dimension expansion via shape rearrangement and then leverage a convolutional block to elaborate the channel perspective. After that, we devise N_{enc} consecutive diffusion blocks (denoted as Diff. Block) utilizing deconvolutions and smoothly diffuse the feature elements that represent m to the same dimension as the width and height of I . Similarly, a series of N_{enc} SE Blocks is promoted for the preparation of watermarking.

Image Reconstruction. Lastly, features of I and m are concatenated with respect to the channel dimension followed by a convolutional block and a vanilla CNN layer to reconstruct the image I_{rec} that is visually identical to I .

3.4. Watermark Recovery

Manipulation Pools. In real-life scenarios, images inevitably suffer degradation by common post-processing operations and noises such as compression and blurring upon uploading and spreading on social media. Therefore, to sat-

isfy the objectives, as shown in Fig. 1, we construct two manipulation pools, P_{common} and P_{swap} , to supervise the proposed framework. On the one hand, the common manipulation pool P_{common} includes the benign post-processing operations that are commonly seen in the real world. On the other hand, we enclose Deepfake face swapping models in the face swapping pool P_{swap} to preserve watermark robustness when facing malicious attacks.

Decoder. We feed the post-manipulation image to the decoder for watermark recovery. The decoder follows a reverse pipeline of the encoder. In particular, after extracting features back to a large number of channels, we apply N_{se} SE Blocks, where $N_{\text{se}} = N_{\text{dec}} + 3$, to gradually expand the number of channels and seek the determinant elements that hide the watermark information. Then, N_{dec} SE Blocks without channel modification are performed after narrowing down the number of channels. In the end, a convolutional block, a flattening operation, and a linear projection are sequentially applied to recover the watermark m_{rec} .

3.5. Objective Functions

During the training stage, we employ a total of 4 loss functions for guidance, namely, *reconstruction loss*, *recovery loss*, *adversarial loss*, and *generative loss*.

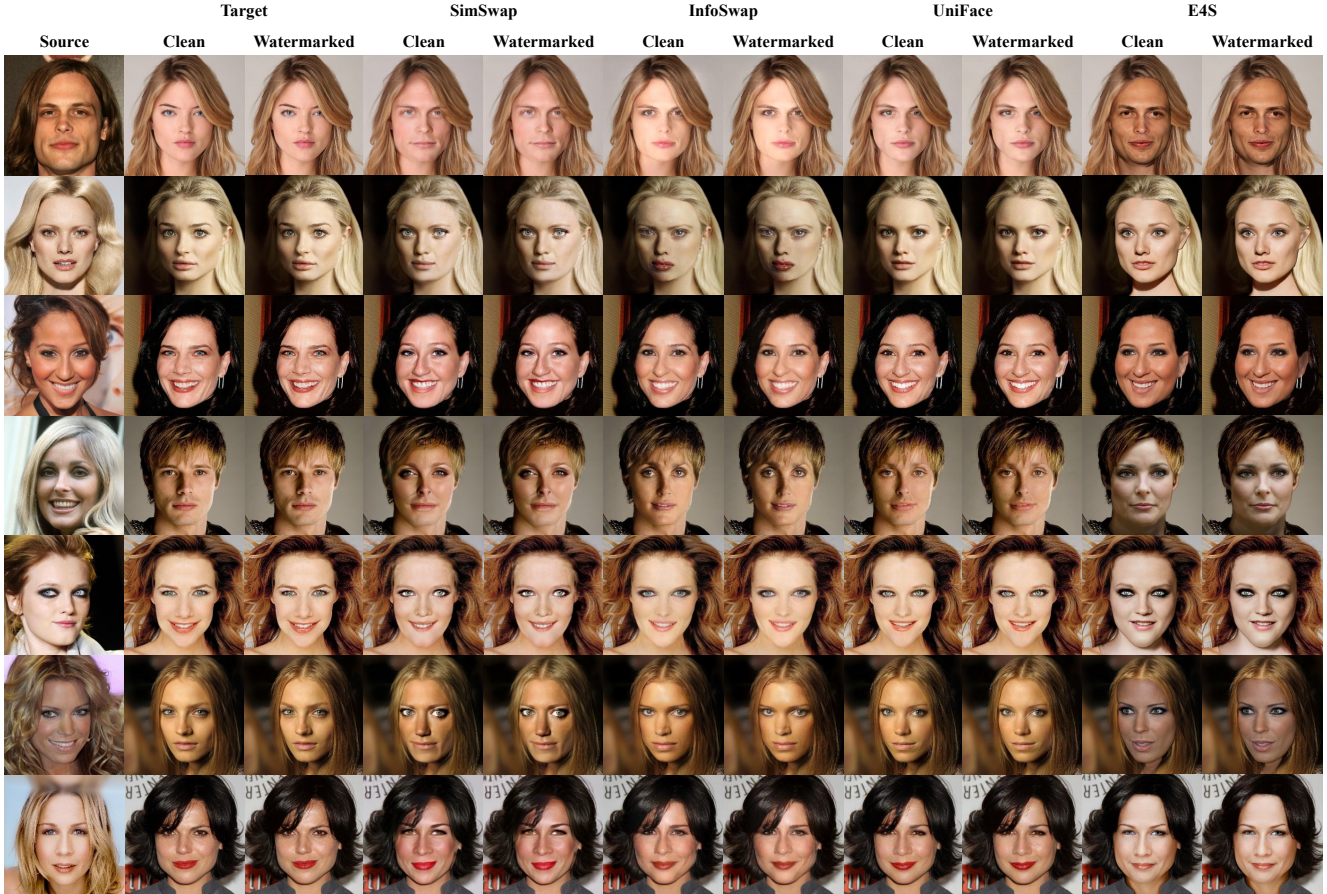


Figure 3. Visual effects of Deepfake face swapping image manipulations on the watermarked images. The first column refers to the source images that provide facial identity for face swapping. Columns 2 and 3 present the raw and watermarked target images. Every two columns of the remaining exhibit the face swapping visualizations on the raw and watermarked target images.

Reconstruction Loss. We embed the watermarks into images and pursue the uttermost similarity between the original and watermarked images by assigning a pixel-wise L_2 constraint on the encoder,

$$L_{\text{enc}} = \|\text{Enc}(\theta_{\text{enc}}, I, m) - I\|_2, \quad (4)$$

where I denotes the clean image before watermarking, m represents the watermark, and θ_{enc} encloses the parameters of the encoder $\text{Enc}(\cdot)$.

Recovery Loss. Similarly, a bit-wise L_2 constraint is applied on the decoder for watermark recovery,

$$L_{\text{dec}} = \|\text{Dec}(\theta_{\text{dec}}, \text{Enc}(\theta_{\text{enc}}, I, m)) - m\|_2, \quad (5)$$

where θ_{dec} refers to the parameters of the decoder $\text{Dec}(\cdot)$. At the same time, the encoder is updated alongside.

Adversarial Loss. Following the convention of robust watermarking [18, 28, 61], a discriminator D with parameters θ_d is applied to improve visual qualities of the images fol-

lowing

$$L_{\text{adv}} = -\mathbb{E}(\log(D(\theta_d, I))) + \mathbb{E}(\log(1 - D(\theta_d, \text{Enc}(\theta_{\text{enc}}, I, m)))). \quad (6)$$

The discriminator is implemented as a binary classifier with N_{dis} convolutional blocks, and it adversarially learns to identify clean and watermarked images on each pair of I and I_{rec} during model supervision.

Generative Loss. When training with the face swapping manipulation pool P_{swap} , we arrange an extra objective using an L_2 constraint to make sure the embedded watermarks do not affect the synthetic results following

$$L_{\text{gen}} = \|G(I, I_s) - G(\text{Enc}(\theta_{\text{enc}}, I, m), I_s)\|_2, \quad (7)$$

where I_s is the image that provides identity information for the face swapping model $G(\cdot)$.

Overall Objective Function. Coefficients λ_{enc} , λ_{dec} , λ_{adv} , and λ_{gen} are assigned to compute the weighted sum in the overall objectives L_{common} and L_{swap} for P_{common} and P_{swap}

Table 1. Quantitative visual quality evaluation of the watermarked images on CelebA-HQ. Information includes model name, image resolution, watermark length, PSNR, and SSIM. The best performance for each resolution is in **bold** and the second best performance is marked with underline.

Model	Resolution	Length	PSNR \uparrow	SSIM \uparrow
HiDDeN [61]	128 \times 128	30	33.26	0.888
MBRS [18]	128 \times 128	30	33.01	0.775
RDA [58]	128 \times 128	100	<u>43.93</u>	<u>0.975</u>
CIN [28]	128 \times 128	30	43.37	0.967
SepMark † [51]	128 \times 128	30	38.51	0.959
ARWGAN [16]	128 \times 128	30	39.58	0.919
Ours	128 \times 128	64	47.39	0.993
AntiForgery [44]	256 \times 256	–	35.62	0.953
CMUA [15]	256 \times 256	–	38.64	0.857
MBRS [18]	256 \times 256	256	<u>44.14</u>	<u>0.969</u>
FaceSigns [31]	256 \times 256	128	36.99	0.889
SepMark † [51]	256 \times 256	128	38.56	0.933
Ours	256 \times 256	128	45.38	0.994

† Statistics adopted from the published paper due to unavailable source code for reproduction.

following

$$L_{\text{common}} = \lambda_{\text{enc}}L_{\text{enc}} + \lambda_{\text{dec}}L_{\text{dec}} + \lambda_{\text{adv}}L_{\text{adv}}, \quad (8)$$

and

$$L_{\text{swap}} = L_{\text{common}} + \lambda_{\text{gen}}L_{\text{gen}}. \quad (9)$$

4. Experiment

4.1. Implementation Details

Datasets. Experiments are conducted on the high-quality CelebA-HQ dataset [19] with 30,000 image samples and 6,217 unique identities following the official split [26] for training, validation, and testing. To further validate the generalization ability, we tested the trained model on the Labeled Faces in the Wild (LFW) dataset [14] with 5,749 unique identities.

Manipulation Pools. P_{common} consists of the following manipulations for both training and testing: Dropout, Resize, Jpeg Compression, Gaussian Noise, Salt and Pepper, Gaussian Blur, and Median Blur. P_{swap} includes SimSwap [5] solely in the training phase and adopts SimSwap, InfoSwap [10], UniFace [52], and E4S [27] with state-of-the-art performance for cross-manipulation evaluation in the testing phase. Since there are various common manipulations to be considered and they only bring noises without modifying the facial contents, we first pre-trained the model using P_{common} for sufficient iterations. Thenceforth, we slowly fine-tuned it with the help of P_{swap} by introducing random images that provide different facial identities for swapping onto I_{rec} .

Parameters. Upon watermark generation, CelebA-HQ is adopted to derive the transform rule ϕ with cutoff value $c = 0.5$, and we set $x_0 = 0.1$, $r = 3.93$, $p = 5$, and $q = 11$ for the constant coefficients in Eqn.(2) and Eqn.(3). We conducted watermark encoding with lengths 64 and 128 for images at 128 \times 128 and 256 \times 256 resolutions, respectively, and we set N_{enc} to 3 and 4, N_{dec} to 1 and 2, and N_{dis} to 3 and 4 for the two resolutions. In this study, we trained the model in two steps. The proposed approach is firstly trained with P_{common} by setting $\lambda_{\text{enc}} = 1$, $\lambda_{\text{dec}} = 10$, and $\lambda_{\text{adv}} = 0.01$ with a learning rate of $1e - 3$ to guarantee the promising watermark recovery performance regarding common manipulations. Then, the trained model is further tuned on SimSwap by setting $\lambda_{\text{enc}} = 10$, $\lambda_{\text{dec}} = 1$, $\lambda_{\text{adv}} = 0.01$, and $\lambda_{\text{gen}} = 5$ with a lower learning rate of $1e - 5$. This process mildly adjusts the framework to stay robust when facing both common and face swapping manipulations. Adam optimizers [21] are adopted through the entire training pipeline for each model component. Our model is implemented using PyTorch on 4 Tesla V100 GPUs with a batch size of 32.

4.2. Experiment on CelebA-HQ

In this section, experiments are conducted on the testing set of CelebA-HQ. Since no existing work has performed detection and source tracing on face swapping images using a single watermark to our knowledge, we selected the robust watermarking frameworks (HiDDeN [61], MBRS [18], and CIN [28]), proactive robust Deepfake watermarking frameworks (RDA [58], SepMark [51], and ARWGAN [16]), proactive semi-fragile Deepfake watermarking frameworks (FaceSigns [31]), and proactive Deepfake distortion frameworks (AntiForgery [44] and CMUA [15]) for comparison. For fairness, the publicly available trained model weights that correspond to optimal performance are directly adopted. Statistics of the recent proactive separable watermark framework, SepMark¹ [51], are copied from the published paper due to unavailable source code.

4.2.1 Qualitative Evaluation

We visualized randomly drafted images to validate the visual quality of the watermarked images. As exhibited in Fig. 2, despite knowing the existence of the watermarks, differences between the raw and watermarked images in the first and second columns, respectively, are visually imperceptible. Starting from column 3, we illustrated the visual effects of the common manipulations on the watermarked images, one for each column. In Fig. 3, the face swapping

¹SepMark [51] is only compared in Table 1 because the reported results are on CelebA-HQ, but the parameters are unrevealed for the common manipulations, leading to unavailability in maintaining a fair comparison in the remaining experiments.

Table 2. Quantitative comparison on CelebA-HQ at 128 and 256 resolutions regarding the bit-wise recovery accuracy of the watermarks under common manipulations and malicious face swapping manipulations. The best performance for each resolution is in **bold** and the second best performance is marked with underscore.

Manipulations	HiDDeN	MBRS	RDA	CIN	ARWGAN	Ours	MBRS	FaceSigns	Ours
	[61] 128 × 128	[18] 128 × 128	[58] 128 × 128	[28] 128 × 128	[16] 128 × 128	128 × 128	[18] 128 × 128	[31] 128 × 128	256 × 256
Dropout	82.44%	100.00%	94.76%	100.00%	97.25%	99.99%	99.19%	55.36%	99.99%
Resize	82.01%	100.00%	99.94%	99.17%	93.73%	100.00%	100.00%	98.63%	99.08%
Jpeg	67.84%	99.49%	66.85%	96.86%	57.42%	99.48%	99.69%	82.64%	99.99%
GaussianNoise	51.36%	99.60%	60.18%	86.00%	53.45%	98.63%	58.31%	53.61%	99.97%
SaltPepper	52.30%	99.37%	66.62%	93.95%	64.55%	95.54%	65.33%	73.95%	97.54%
GaussianBlur	73.04%	100.00%	99.95%	100.00%	85.22%	100.00%	72.05%	98.68%	97.93%
MedBlur	82.72%	100.00%	99.98%	97.03%	96.66%	100.00%	98.06%	99.86%	99.01%
Average	70.24%	99.78%	84.04%	96.14%	78.33%	<u>99.09%</u>	<u>84.66%</u>	80.39%	99.07%
SimSwap [5]	50.02%	49.98%	50.00%	50.28%	52.06%	99.99%	50.00%	49.74%	99.98%
InfoSwap [10]	50.07%	50.82%	50.01%	50.60%	47.94%	99.31%	50.71%	50.00%	99.73%
UniFace [52]	54.98%	50.22%	71.15%	46.01%	59.30%	99.57%	49.98%	50.59%	94.86%
E4S [27]	49.19%	50.07%	63.03%	50.55%	49.81%	93.19%	50.07%	49.73%	93.33%
Average	51.07%	50.27%	<u>58.55%</u>	49.36%	52.28%	98.02%	<u>50.19%</u>	50.02%	96.98%

Table 3. Quantitative visual quality evaluation of the watermarked images on LFW. Information includes model name, image resolution, watermark length, PSNR, and SSIM. The best performance for each resolution is in **bold** and the second best performance is marked with underscore.

Model	Resolution	Length	PSNR \uparrow	SSIM \uparrow
HiDDeN [61]	128 × 128	30	33.27	0.883
MBRS [18]	128 × 128	30	32.78	0.761
RDA [58]	128 × 128	100	42.71	0.959
CIN [28]	128 × 128	30	<u>42.89</u>	<u>0.982</u>
ARWGAN [16]	128 × 128	30	39.94	0.926
Ours	128 × 128	64	46.00	0.993
MBRS [18]	256 × 256	256	<u>45.37</u>	<u>0.969</u>
FaceSigns [31]	256 × 256	128	38.23	0.910
Ours	256 × 256	128	45.42	0.994

effects are exhibited in every two columns starting from column 4. The source images that provide the desired synthetic facial identities for each row are placed in the first column. Columns 2 and 3 display the raw and watermarked target images, while every pair of the remaining columns illustrates the face swapping results on the raw and watermarked target images, respectively. It is worth noting that no distortion can be observed in the face swapping results using watermarked target images. In other words, the encoded watermarks do not affect the visual qualities of the synthetic faces, preserving the possible benign usages of Deepfake face swapping in the industry.

4.2.2 Quantitative Evaluation

In this section, we quantitatively evaluated the visual qualities of watermarked images and the watermark recovery accuracies after common and face swapping manipulations.

Visual Quality. We employed the average peak signal-to-noise ratio (PSNR) and structural similarity index measure (SSIM) [49] between the raw and watermarked images to evaluate the visual quality of watermarked images. As Table 1 reports, while the goal of embedding watermarks into raw images imperceptibly stands for all contrastive methods, our proposed approach achieves the state-of-the-art visual quality in terms of PSNR and SSIM at both resolution levels. Meanwhile, it can be observed that although pursuing the same objective in visual quality, the proactive distortion models, AntiForgery [44] and CMUA [15], have revealed relatively unsatisfactory performance since the noises and perturbations are directly added to raw images while watermarking approaches execute image reconstructions.

Watermark Recovery on Common Manipulations. The watermarks are represented via binary values, and the bit-wise accuracy of the recovered watermark is computed by comparing it to the original watermark following

$$\text{ACC}(m_{\text{rec}}, m) = \frac{l - d_{\text{ham}}(m_{\text{rec}}, m)}{l}, \quad (10)$$

where d_{ham} computes the hamming distance [43] between the recovered and original watermarks m_{rec} and m , and l refers to the watermark length. In the experiment, each type of manipulation in P_{common} and P_{swap} is performed on the watermarked image I_{rec} before extracting the watermark via the decoder.

Table 4. Quantitative comparison on LFW at 128 and 256 resolutions regarding the bit-wise recovery accuracy of the watermarks under common manipulations and malicious face swapping manipulations. The best performance for each resolution is in **bold** and the second best performance is marked with underscore.

Manipulations	HiDDeN	MBRS	RDA	CIN	ARWGAN	Ours	MBRS	FaceSigns	Ours
	[61] 128 × 128	[18] 128 × 128	[58] 128 × 128	[28] 128 × 128	[16] 128 × 128	128 × 128	[18] 128 × 128	[31] 128 × 128	256 × 256
Dropout	82.84%	99.99%	89.72%	100.00%	97.28%	99.96%	99.30%	56.45%	99.97%
Resize	81.97%	100.00%	99.89%	99.98%	95.07%	99.99%	100.00%	98.91%	98.16%
Jpeg	56.17%	99.42%	66.77%	97.06%	70.86%	99.38%	99.08%	75.64%	99.99%
GaussianNoise	51.30%	99.80%	60.83%	87.54%	53.11%	99.63%	55.61%	59.90%	99.92%
SaltPepper	52.93%	99.63%	67.31%	91.71%	62.96%	95.89%	61.15%	67.99%	95.99%
GaussianBlur	72.89%	100.00%	99.88%	99.99%	86.39%	99.99%	73.93%	99.01%	97.11%
MedBlur	82.35%	99.99%	99.98%	99.98%	96.93%	99.99%	99.38%	99.91%	98.13%
Average	68.63%	99.83%	83.48%	96.61%	80.37%	<u>99.26%</u>	<u>84.06%</u>	79.69%	98.47%
SimSwap [5]	49.96%	49.92%	50.04%	50.25%	50.00%	99.37%	50.04%	49.77%	99.96%
InfoSwap [10]	50.06%	50.04%	50.10%	50.95%	50.86%	98.69%	50.23%	49.91%	98.67%
UniFace [52]	53.74%	49.78%	70.37%	49.92%	59.16%	98.48%	50.18%	52.25%	97.06%
E4S [27]	49.34%	50.08%	67.78%	50.22%	48.64%	97.27%	49.99%	50.15%	97.00%
Average	50.77%	49.96%	<u>59.57%</u>	50.33%	52.18%	98.45%	50.11%	<u>50.52%</u>	98.17%

The watermark recovery performance in the comparative experiment is reported in Table 2. Specifically, considering the common manipulations, our method outperforms HiDDeN [61], RDA [58], CIN [28], and ARWGAN [16] at the 128×128 resolution with a better average accuracy, and our performance is competitive against MBRS [18] with an acceptable average accuracy above 99%, achieving the second best statistic. However, it can be observed from Table 1 that MBRS heavily suffers visual quality issues with unsatisfactory PSNR and SSIM values (33.01 and 0.775) in order to achieve the best bit-wise watermark recovery accuracy in Table 2. As for the 256×256 resolution, we reached an average accuracy of 99.07% on the common manipulations, outperforming the existing state-of-the-art methods. On the contrary, although accomplishes reasonable visual quality as listed in Table 1, MBRS experiences a large performance damping on the common manipulations in Table 2 with respect to the watermark recovery accuracy compared to the 128×128 resolution version.

Watermark Recovery on Face Swapping. In this paper, the face swapping manipulation pool contains merely SimSwap [5] in the training phase, and we validated the watermark recovery performance for both in- and cross-manipulation settings by introducing other recent state-of-the-art face swapping algorithms, InfoSwap [10], UniFace [52], and E4S [27], in the testing phase. As shown in Table 2, our model consistently recovers the desired watermark messages at average accuracies of 98.02% and 96.98% for 128×128 and 256×256 resolutions, respectively, while HiDDeN, MBRS, CIN, and ARWGAN all obtain accuracies around 50% and RDA has accuracies below 75% against all synthetic models. Moreover,

it can be concluded from the cross-manipulation tests on unseen synthetic models that by simply tuning with SimSwap, the hidden watermarks are pleasantly maintained by our method since the goals for different face swapping algorithms are identical. Meanwhile, the semi-fragile watermarking framework, FaceSigns [31], although obtains low watermark recovery accuracies as designed when facing synthetic manipulations that are expected to destroy the embedded watermarks, its performance regarding the common manipulations is unexpectedly unsatisfactory besides illustrating low visual quality as reported in Table 1, leading to an average recovery accuracy of 80.39%.

Discussion. In general, Salt and Pepper and Gaussian Noise are the most challenging common manipulations that cause fluctuations in the watermark recovery accuracies for all watermarking algorithms as summarized in Table 2. This is consistent with the visualization results in Fig. 2 (col. 6 & 9) such that these two manipulations add a plethora of perceivable noises to the images and thus heavily jeopardize the hidden watermarks. On the other hand, the contrastive robust watermarking frameworks fail to maintain robustness when facing the state-of-the-art face swapping models. As a result, our proposed model is the only one that maintains the bit-wise watermark recovery accuracies above 95% for all common manipulations and above 90% for all face swapping manipulations, while the contrastive methods are heavily affected by at least one of the manipulations.

4.3. Cross-Dataset Experiment

We further evaluated our watermarking framework on an unseen dataset, Labeled Faces in the Wild (LFW) [14], re-

Table 5. Deepfake detection performance in AUC scores against different face swapping algorithms on CelebA-HQ at 128×128 and 256×256 resolutions. The last row evaluates the detection performance on a mixture of all face swapping algorithms. The best performance at each resolution is in **bold** and the second best performance is marked with underscore.

Resolution	Xception [53]		SBI [39]		RECCE [4]		CADD [7]		Ours	
	128	256	128	256	128	256	128	256	128	256
SimSwap [5]	39.73%	71.15%	<u>75.30%</u>	<u>88.94%</u>	60.37%	69.01%	55.91%	87.66%	98.49%	98.19%
InfoSwap [10]	60.82%	65.50%	<u>85.11%</u>	<u>80.50%</u>	55.51%	52.13%	48.29%	61.39%	99.02%	99.52%
UniFace [52]	71.49%	70.34%	72.45%	79.41%	61.58%	67.35%	<u>82.16%</u>	<u>82.73%</u>	99.99%	98.99%
E4S [27]	43.40%	53.70%	63.63%	61.05%	60.88%	47.19%	<u>64.93%</u>	<u>73.13%</u>	97.71%	98.70%
Mixed	49.71%	63.04%	<u>75.96%</u>	<u>80.05%</u>	62.84%	57.13%	64.41%	72.52%	98.66%	98.97%
FF++ [38]	97.60%		90.50%		96.81%		95.57%		-	

guarding the generalization ability. Performance evaluation with respect to the visual quality is listed in Table 3. Similar results as in Table 1 can be summarized even on a different dataset. In particular, for the 128×128 resolution, our approach consistently exhibits substantial performance advantages over the comparative ones. As for the 256×256 resolution, MBRS [18] and our approach both have executed watermarking with promising visual qualities while FaceSigns [31] fails to do so.

Meanwhile, as listed in Table 4, the challenging manipulations concluded in Section 4.2 consistently lead to unsatisfactory bit-wise watermark recovery accuracies in this section. Consequently, although slightly affected by Salt and Pepper (95.89% and 95.99%) and Gaussian Blur (99.99% and 97.11%) at 128×128 and 256×256 resolutions, respectively, we successfully maintained state-of-the-art accuracies above 95% for all common and face swapping manipulations.

Furthermore, obvious accuracy declines of our approach on UniFace [52] at the 256×256 resolution and on E4S [27] at both resolutions can be observed in Table 2 and Table 4 on CelebA-HQ and LFW. Besides the challenges caused by the cross-manipulation setting, the former is mainly due to the setting of accepting only half-precision floating-point inputs by UniFace. Although the synthetic pipeline is unaffected, this can lead to discrepancies in the watermark recovery process at higher resolution levels because of information loss. On the other hand, the performance on E4S is affected by adopting an extra color channel, alpha, during image synthesis, which reduces the watermark feature density in the face swapped images, leading to a relatively lower watermark recovery accuracy.

4.4. Watermark Collision Check

As introduced in Section 3.2, the binary identity perceptual watermarks are derived from identity embeddings generated via well-designed face recognition tools². To validate

²<https://github.com/serengil/deepface>

the claim that the identity perceptual watermarks retain the collision-free characteristic of the original identity embeddings, we performed collision checks at different watermark lengths on CelebA-HQ [19] and LFW [14]. In specific, for the sets of watermarks M_i and M_j of a pair of arbitrary identities i and j , the following statement stands,

$$\forall x \in M_i \forall y \in M_j (x \neq y). \quad (11)$$

In other words, identical watermarks are not allowed to be derived from images that belong to different identities.

In this paper, images from CelebA-HQ with 6,217 unique identities are adopted to establish ϕ and produce watermarks following the pipeline in Section 3.2. Thereafter, the watermarks of images in LFW with 5,749 unseen identities are derived following the fixed rule accordingly.

As a result, there is no collision in the experiment for CelebA-HQ and LFW at both 128×128 and 256×256 resolutions in our collision check. Meanwhile, upon passing the collision check even though not seeing the identities in LFW when defining ϕ , it can be concluded that the number of unique identities in CelebA-HQ is sufficient to avoid the potential bias, and the cross-dataset performance is therefore preserved.

4.5. Deepfake Detection

In this section, the Deepfake detection task is proactively achieved by evaluating the recovered watermark m_{rec} . In specific, for a target image I with identity t to be proactively protected with identity perceptual watermark m , the watermarked image I_{rec} is firstly derived via the encoder of our framework. Then, when a face swapping algorithm from P_{swap} is applied on I_{rec} to generate I_{fake} with identity s , the identity perceptual watermark m_s is derived based on the image content of I_{fake} , and the robust watermark is also recovered, denoted as m_{rec} , via the decoder of our framework. In the end, the two watermarks, m_s and m_{rec} , are compared bit-wisely and the falsification can be addressed based on their matching rate.

Table 6. Robustness ablation test on common manipulations for easier and harder parameter values that are unseen during training. The bit-wise watermark recovery accuracies are reported. Long common manipulation names are abbreviated.

Difficulty	Dropout (r)		Resize (r)		Jpeg (Q)		GNoise (μ, σ)		S&P (r)		GBlur (σ, k)		MBlur (k)	
	r	Acc	r	Acc	Q	Acc	μ, σ	Acc	r	Acc	σ, k	Acc	k	Acc
Easy	0.3	99.99%	0.3	100.00%	70	100.00%	0, 0.05	100.00%	0.03	99.76%	1, 1	100.00%	1	100.00%
Regular	0.5	99.99%	0.5	100.00%	50	99.48%	0, 0.1	98.63%	0.05	95.54%	2, 3	100.00%	3	100.00%
Hard	0.7	99.46%	0.7	99.82%	30	99.38%	0, 0.2	93.24%	0.07	94.19%	3, 5	98.08%	5	99.50%

Since the comparative proactive watermarking approaches do not assign semantics to their watermarks, Deepfake detection cannot be accomplished without knowing the matched watermark for each image in advance, and this is usually unavailable in real-life scenarios. Meanwhile, the unsatisfactory watermark recovery accuracies in Section 4.2 suggest that the detection performance evaluation can be trivial for them. Therefore, in this experiment, we adopted several state-of-the-art passive Deepfake detectors in recent years for comparison, namely, SBIs [39], RECCE [4], and CADDM [7]. We also consider the popular milestone detector, Xception³ [38], as one of the contrastive algorithms. All the models are utilized with their published weights corresponding to the optimal performance.

Since the accuracy metric requires a fixed threshold value which can lead to biases due to data distributions, we employed the area under the receiver operating characteristic (ROC) curve (AUC) score to evaluate the detection performance based on the matching rate. In a nutshell, a high AUC score demonstrates the probability that a random positive sample scores higher than a random negative sample from the testing set, in other words, the ability of the classifier to distinguish between real and fake samples. The experiment is conducted on CelebA-HQ at 128×128 and 256×256 resolutions by testing against each face swapping model in P_{swap} and a mixture⁴ of them. To establish a balanced ratio for real and fake samples, the real images in CelebA-HQ are leveraged after randomly applying common manipulations from P_{common} .

The detection performance in AUC scores is demonstrated in Table 5. It can be observed that, although exhibit reasonable detection performance in lab-controlled scenarios, in this experiment, the passive detectors generally come up with poor AUC scores of at most 88.94%. Moreover, various statistics are observed below 70% regarding each passive model, demonstrating substantial fluctuations in the detection performance. We also listed their performance on the training dataset, FaceForensics++ [38] (FF++) dataset, for a reference. As a result, huge performance damping

³The well-trained model weights are adopted from a recent benchmark study [53].

⁴When conducting this experiment, samples are equally and randomly drawn for each synthetic algorithm to match up the same total quantity as the real ones.

can be concluded for the passive detectors since the face swapping models are unseen and can generate faces with imperceptible detectable artifacts. Meanwhile, the passive detectors trained in lab-controlled scenarios fail to stay robust when facing common manipulations on the real samples that simulate the real-life scenarios.

On the contrary, our proposed approach successfully retains promising AUC scores above 97% for both seen and unseen face swapping manipulations at both resolutions. This implies that the matching rates between m_s and m_{rec} for images after common manipulations (real) are consistently higher than those for images after face swapping manipulations (fake). In other words, our identity perceptual watermarking framework not only robustly survives via image manipulations, but favorably distinguishes real and fake samples with respect to the changes in facial identities. As a result, for a mixture of all four manipulations including three unseen ones, our approach retains satisfactory detection performance at 98.66% and 98.97% at 128×128 and 256×256 resolutions, respectively, demonstrating superior generalization ability.

4.6. Ablation Study on Common Manipulations

In this paper, following the convention of steganography, we picked the common manipulations that best imitate the unavoidable image quality degradation of posting and spreading in real-life scenarios and set the parameter values with considerable difficulties. Particularly, the parameters are set equal to or harder than the early work [18, 28, 61] in our experiments. In this section, to further validate the robustness of the proposed watermarking framework, we conducted ablation testing sessions on CelebA-HQ at the 256×256 resolution with easier and harder parameters that are unseen during training for the common manipulations, respectively. As a result, in addition to the outstanding performance reported in Sections 4.2 and 4.3, Table 6 implies that the robustness is completely guaranteed for common manipulations with easier parameter values, and it is also only slightly affected in harder conditions, with all accuracies still above 90%. In conclusion, the potential effects of common manipulations at different difficulty levels are trivial with respect to the robustness of our proposed approach.

5. Conclusion

In this paper, we propose a robust identity perceptual watermarking framework that proactively defends against malicious Deepfake face swapping. By securely assigning identity semantics to the watermarks, our approach concurrently accomplishes detection and source tracing with a single robust watermark for the first time. Meanwhile, the confidentiality is guaranteed by devising an unpredictable chaotic encryption system on the identity perceptual watermarks. Extensive experimental results have proved that our method is robust when facing both common and malicious manipulations on the watermarked images even under cross-dataset settings. Moreover, by leveraging a single Deepfake face swapping algorithm for fine-tuning, we are able to preserve promising cross-manipulation performance against unseen face swapping algorithms. The AUC scores of 98.66% and 98.97% at 128×128 and 256×256 resolutions further prove the promising detection ability of our approach on Deepfake face swapping, significantly outperforming the state-of-the-art passive detectors.

Admittedly, since the watermarks are identity perceptual, the proposed framework is unable to detect face re-enactment manipulations that modify facial expressions and poses but retain facial identities. Our future work will focus on designing a unified framework to proactively defend against both face swapping and face re-enactment manipulations by analyzing and introducing the corresponding facial attribute features.

References

- [1] Turker Akyuz and Ibrahim Sogukpinar. Packet marking with distance based probabilities for ip traceback. In *2009 First International Conference on Networks & Communications*, pages 433–438, 2009. 2
- [2] Shivangi Aneja, Lev Markhasin, and Matthias Nießner. Tafim: Targeted adversarial attacks against facial image manipulations. In *Eur. Conf. Comput. Vis.*, pages 58–75, 2022. 2
- [3] Nicolas Beuve, Wassim Hamidouche, and Olivier Déforges. Waterloo: Protect images from deepfakes using localized semi-fragile watermark. In *Int. Conf. Comput. Vis. Worksh.*, pages 393–402, 2023. 1
- [4] Junyi Cao, Chao Ma, Taiping Yao, Shen Chen, Shouhong Ding, and Xiaokang Yang. End-to-end reconstruction-classification learning for face forgery detection. In *IEEE Conf. Comput. Vis. Pattern Recog.*, pages 4113–4122, 2022. 10, 11
- [5] Renwang Chen, Xuanhong Chen, Bingbing Ni, and Yanhao Ge. Simswap: An efficient framework for high fidelity face swapping. In *ACM Int. Conf. Multimedia*, page 2003–2011, New York, NY, USA, 2020. Association for Computing Machinery. 7, 8, 9, 10
- [6] I. J. Cox, M. L. Miller, and J. A. Bloom. *Digital Watermarking*. Morgan Kaufmann Publishers, San Francisco, 2002. 4
- [7] Shichao Dong, Jin Wang, Renhe Ji, Jiajun Liang, Haoqiang Fan, and Zheng Ge. Implicit identity leakage: The stumbling block to improving deepfake detection generalization. In *IEEE Conf. Comput. Vis. Pattern Recog.*, pages 3994–4004, 2023. 10, 11
- [8] Han Fang, Zhaoyang Jia, Zehua Ma, Ee-Chien Chang, and Weiming Zhang. Pimog: An effective screen-shooting noise-layer simulation for deep-learning-based watermarking network. In *ACM Int. Conf. Multimedia*, page 2267–2275, 2022. 2
- [9] Guan hao Gan, Yiming Li, Dongxian Wu, and Shu-Tao Xia. Towards robust model watermark via reducing parametric vulnerability. *Int. Conf. Comput. Vis.*, 2023. 2
- [10] Gege Gao, Huaibo Huang, Chaoyou Fu, Zhaoyang Li, and Ran He. Information bottleneck disentanglement for identity swapping. In *IEEE Conf. Comput. Vis. Pattern Recog.*, pages 3403–3412, 2021. 7, 8, 9, 10
- [11] Ziwen He, Wei Wang, Weinan Guan, Jing Dong, and Tieniu Tan. Defeating deepfakes via adversarial visual reconstruction. In *ACM Int. Conf. Multimedia*, page 2464–2472. Association for Computing Machinery, 2022. 2
- [12] Jie Hu, Li Shen, and Gang Sun. Squeeze-and-excitation networks. In *IEEE Conf. Comput. Vis. Pattern Recog.*, pages 7132–7141, 2018. 4
- [13] B. Huang, Z. Wang, J. Yang, J. Ai, Q. Zou, Q. Wang, and D. Ye. Implicit identity driven deepfake face swapping detection. In *IEEE Conf. Comput. Vis. Pattern Recog.*, pages 4490–4499, 2023. 1, 2
- [14] Gary B. Huang, Marwan Mattar, Honglak Lee, and Erik Learned-Miller. Learning to align from scratch. In *Adv. Neural Inform. Process. Syst.*, 2012. 7, 9, 10
- [15] Hao Huang, Yongtao Wang, Zhaoyu Chen, Yuze Zhang, Yuheng Li, Zhi Tang, Wei Chu, Jingdong Chen, Weisi Lin, and Kai-Kuang Ma. Cmu-watermark: A cross-model universal adversarial watermark for combating deepfakes. *AAAI*, 36(1):989–997, 2022. 1, 2, 7, 8
- [16] Jiangtao Huang, Ting Luo, Li Li, Gaobo Yang, Haiyong Xu, and Chin-Chen Chang. Arwgan: Attention-guided robust image watermarking model based on gan. *IEEE Transactions on Instrumentation and Measurement*, 72:1–17, 2023. 2, 3, 7, 8, 9
- [17] Qidong Huang, Jie Zhang, Wenbo Zhou, Weiming Zhang, and Nenghai Yu. Initiative defense against facial manipulation. *AAAI*, 35(2):1619–1627, 2021. 2
- [18] Zhaoyang Jia, Han Fang, and Weiming Zhang. Mbrs: Enhancing robustness of dnn-based watermarking by mini-batch of real and simulated jpeg compression. In *ACM Int. Conf. Multimedia*, 2021. 2, 6, 7, 8, 9, 10, 11
- [19] Tero Karras, Timo Aila, Samuli Laine, and Jaakko Lehtinen. Progressive growing of GANs for improved quality, stability, and variation. In *Int. Conf. Learn. Represent.*, 2018. 7, 10
- [20] Hyungseok Kim, Eunjin Kim, Seungmo Kang, and Huy Kang Kim. Network forensic evidence generation and verification scheme (nfevgs). *Telecommunication Systems*, 60:261–273, 2015. 2
- [21] Diederik P. Kingma and Jimmy Ba. Adam: A method for stochastic optimization. In *Int. Conf. Learn. Represent.*, 2015. 7

- [22] Lingzhi Li, Jianmin Bao, Ting Zhang, Hao Yang, Dong Chen, Fang Wen, and Baining Guo. Face x-ray for more general face forgery detection. In *IEEE Conf. Comput. Vis. Pattern Recog.*, pages 5000–5009, 2020. 1, 2
- [23] Li Li, Yu Bai, Ching-Chun Chang, Yunyuan Fan, Wei Gu, and Mahmoud Emam. Anti-pruning multi-watermarking for ownership proof of steganographic autoencoders. *Journal of Information Security and Applications*, 76:103548, 2023. 2
- [24] Yuenan Li, Dongdong Wang, and Linlin Tang. Robust and secure image fingerprinting learned by neural network. *IEEE Trans. Circuit Syst. Video Technol.*, 30(2):362–375, 2020. 3
- [25] Honggu Liu, Xiaodan Li, Wenbo Zhou, Han Fang, Paolo Bestagini, Weiming Zhang, Yuefeng Chen, Stefano Tubaro, Nenghai Yu, Yuan He, and Hui Xue. Bifpro: A bidirectional facial-data protection framework against deepfake. In *ACM Int. Conf. Multimedia*, page 7075–7084, 2023. 1
- [26] Ziwei Liu, Ping Luo, Xiaogang Wang, and Xiaoou Tang. Deep learning face attributes in the wild. In *Int. Conf. Comput. Vis.*, 2015. 7
- [27] Zhian Liu, Maomao Li, Yong Zhang, Cairong Wang, Qi Zhang, Jue Wang, and Yongwei Nie. Fine-grained face swapping via regional gan inversion. In *IEEE Conf. Comput. Vis. Pattern Recog.*, pages 8578–8587, 2023. 7, 8, 9, 10
- [28] Rui Ma, Mengxi Guo, Yi Hou, Fan Yang, Yuan Li, Huizhu Jia, and Xiaodong Xie. Towards blind watermarking: Combining invertible and non-invertible mechanisms. In *ACM Int. Conf. Multimedia*, pages 1532–1542, 2022. 2, 3, 6, 7, 8, 9, 11
- [29] Robert Matthews. On the derivation of a “chaotic” encryption algorithm. *Cryptologia*, 13(1):29–42, 1989. 4
- [30] Aakash Varma Nadimpalli and Ajita Rattani. Proactive deepfake detection using gan-based visible watermarking. *ACM Trans. Multimedia Comput. Commun. Appl.*, 2023. 1
- [31] Paarth Neekhara, Shehzeen Hussain, Xinqiao Zhang, Ke Huang, Julian McAuley, and Farinaz Koushanfar. Facesigns: Semi-fragile neural watermarks for media authentication and countering deepfakes. *CoRR*, 2022. 1, 3, 7, 8, 9, 10
- [32] Yuval Nirkin, Lior Wolf, Yosi Keller, and Tal Hassner. Deepfake detection based on discrepancies between faces and their context. *IEEE Trans. Pattern Anal. Mach. Intell.*, 44(10):6111–6121, 2022. 2
- [33] Utkarsh Ojha, Yuheng Li, and Yong Jae Lee. Towards universal fake image detectors that generalize across generative models. In *IEEE Conf. Comput. Vis. Pattern Recog.*, 2023. 1, 2
- [34] Karl Pearson. On lines and planes of closest fit to systems of points in space. *The London, Edinburgh, and Dublin Philosophical Magazine and Journal of Science*, 2:559–572, 1901. 3
- [35] Tong Qiao, Shichuang Xie, Yanli Chen, Florent Reiraint, and Xiangyang Luo. Fully unsupervised deepfake video detection via enhanced contrastive learning. *IEEE Trans. Pattern Anal. Mach. Intell.*, pages 1–18, 2024. 1
- [36] Chuan Qin, Enli Liu, Guorui Feng, and Xinpeng Zhang. Perceptual image hashing for content authentication based on convolutional neural network with multiple constraints. *IEEE Trans. Circuit Syst. Video Technol.*, 31(11):4523–4537, 2021. 3
- [37] Nataniel Ruiz, Sarah Adel Bargal, and Stan Sclaroff. Disrupting deepfakes: Adversarial attacks against conditional image translation networks and facial manipulation systems. In *Eur. Conf. Comput. Vis. Worksh.*, pages 236–251, 2020. 2
- [38] Andreas Rössler, Davide Cozzolino, Luisa Verdoliva, Christian Riess, Justus Thies, and Matthias Niessner. Faceforensics++: Learning to detect manipulated facial images. In *Int. Conf. Comput. Vis.*, pages 1–11, 2019. 1, 2, 10, 11
- [39] Kaede Shiohara and Toshihiko Yamasaki. Detecting deepfakes with self-blended images. In *IEEE Conf. Comput. Vis. Pattern Recog.*, pages 18720–18729, 2022. 10, 11
- [40] Matthew Tancik, Ben Mildenhall, and Ren Ng. Stegastamp: Invisible hyperlinks in physical photographs. In *IEEE Conf. Comput. Vis. Pattern Recog.*, pages 2114–2123, 2020. 2
- [41] Andrew Tirkel, G.A. Rankin, Ron van Schyndel, W. Ho, N. Mee, and C. Osborne. Electronic watermark. In *Digital Image Computing, Technology and Applications*, 1994. 2
- [42] Sonam Tyagi, Harsh Vikram Singh, Raghav Agarwal, and Sandeep Kumar Gangwar. Digital watermarking techniques for security applications. In *2016 International Conference on Emerging Trends in Electrical Electronics & Sustainable Energy Systems (ICETEESES)*, pages 379–382, 2016. 4
- [43] William M. Waggner. *Pulse Code Modulation Techniques*. Springer, 1995. 8
- [44] Run Wang, Ziheng Huang, Zhikai Chen, Li Liu, Jing Chen, and Lina Wang. Anti-forgery: Towards a stealthy and robust deepfake disruption attack via adversarial perceptual-aware perturbations. In *IJCAI*, pages 761–767, 2022. 1, 2, 7, 8
- [45] Sheng-Yu Wang, Oliver Wang, Richard Zhang, Andrew Owens, and Alexei A Efros. Cnn-generated images are surprisingly easy to spot...for now. In *IEEE Conf. Comput. Vis. Pattern Recog.*, 2020. 1
- [46] Tianyi Wang and Kam Pui Chow. Noise based deepfake detection via multi-head relative-interaction. *AAAI*, 37(12):14548–14556, 2023. 1
- [47] Tianyi Wang, Xin Liao, Kam Pui Chow, Xiaodong Lin, and Yinglong Wang. Deepfake detection: A comprehensive study from the reliability perspective. *CoRR*, 2023. 1
- [48] Xueyu Wang, Jiajun Huang, Siqi Ma, Surya Nepal, and Chang Xu. Deepfake disrupter: The detector of deepfake is my friend. In *IEEE Conf. Comput. Vis. Pattern Recog.*, pages 14920–14929, 2022. 1, 2
- [49] Zhou Wang, A.C. Bovik, H.R. Sheikh, and E.P. Simoncelli. Image quality assessment: from error visibility to structural similarity. *IEEE Trans. Image Process.*, 13(4):600–612, 2004. 8
- [50] Z. Wang, J. Bao, W. Zhou, W. Wang, and H. Li. Altfreezing for more general video face forgery detection. In *IEEE Conf. Comput. Vis. Pattern Recog.*, pages 4129–4138, 2023. 1, 2
- [51] Xiaoshuai Wu, Xin Liao, and Bo Ou. Sepmark: Deep separable watermarking for unified source tracing and deepfake detection. In *ACM Int. Conf. Multimedia*, 2023. 2, 3, 7
- [52] Chao Xu, Jiangning Zhang, Yue Han, Guanzhong Tian, Xianfang Zeng, Ying Tai, Yabiao Wang, Chengjie Wang, and Yong Liu. Designing one unified framework for high-fidelity face reenactment and swapping. In *Eur. Conf. Comput. Vis.*, pages 54–71, 2022. 7, 8, 9, 10

- [53] Zhiyuan Yan, Yong Zhang, Xinhang Yuan, Siwei Lyu, and Baoyuan Wu. Deepfakebench: A comprehensive benchmark of deepfake detection. In *Adv. Neural Inform. Process. Syst.*, 2023. 10, 11
- [54] P. Yang, Y. Lao, and P. Li. Robust watermarking for deep neural networks via bi-level optimization. In *Int. Conf. Comput. Vis.*, pages 14821–14830, 2021. 2
- [55] Yuankun Yang, Chenyue Liang, Hongyu He, Xiaoyu Cao, and Neil Zhenqiang Gong. Faceguard: Proactive deepfake detection. *CoRR*, 2021. 1, 3
- [56] Chin-Yuan Yeh, Hsi-Wen Chen, Shang-Lun Tsai, and Shang-De Wang. Disrupting image-translation-based deepfake algorithms with adversarial attacks. In *2020 IEEE Winter Applications of Computer Vision Workshops (WACVW)*, pages 53–62, 2020. 2
- [57] Chin-Yuan Yeh, Hsi-Wen Chen, Hong-Han Shuai, De-Nian Yang, and Ming-Syan Chen. Attack as the best defense: Nullifying image-to-image translation gans via limit-aware adversarial attack. In *Int. Conf. Comput. Vis.*, pages 16168–16177, 2021. 2
- [58] Ning Yu, Vladislav Skripniuk, Sahar Abdelnabi, and Mario Fritz. Artificial fingerprinting for generative models: Rooting deepfake attribution in training data. In *Int. Conf. Comput. Vis.*, pages 14448–14457, 2021. 3, 7, 8, 9
- [59] Ning Yu, Vladislav Skripniuk, Dingfan Chen, Larry Davis, and Mario Fritz. Responsible disclosure of generative models using scalable fingerprinting. In *Int. Conf. Learn. Represent.*, 2022. 3
- [60] Hanqing Zhao, Tianyi Wei, Wenbo Zhou, Weiming Zhang, Dongdong Chen, and Nenghai Yu. Multi-attentional deepfake detection. In *IEEE Conf. Comput. Vis. Pattern Recog.*, pages 2185–2194, 2021. 1, 2
- [61] Jiren Zhu, Russell Kaplan, Justin Johnson, and Li Fei-Fei. Hidden: Hiding data with deep networks. In *Eur. Conf. Comput. Vis.*, pages 682–697, 2018. 2, 6, 7, 8, 9, 11